AD-A051 343 R AND D ASSOCIATES MARINA DEL REY CALIF F/G 13/1
BASIC REQUIREMENTS FOR NUCLEAR TESTING OF A HEAT-SINK CONCEPT.(U)
OCT 74 J E WHITENER DNA001-74-C-0139

UNCLASSIFIED RDA-TR-5900-012 DNA-4184F NL

| OF |
AD
A051 343

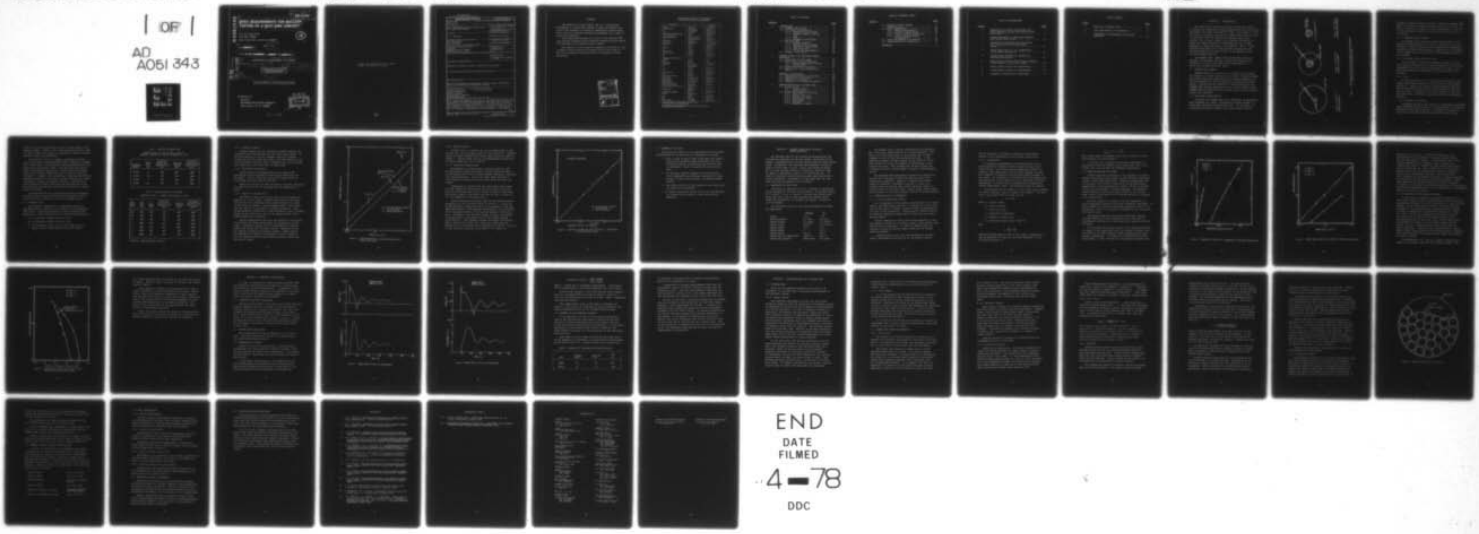

END
DATE
FILMED
4-78
DDC

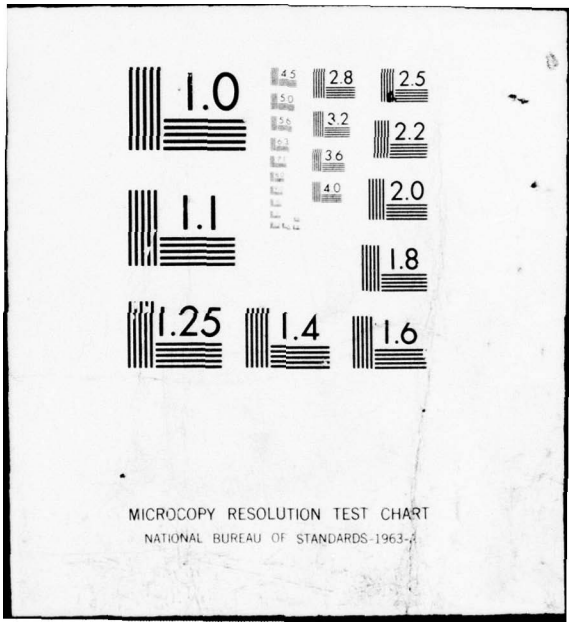
1.0
1.1
1.25
1.4
1.6
1.8
2.0
2.2
2.5
2.8
3.2
3.6
4.0
4.5
5.0
5.6
MICROCOPY RESOLUTION TEST CHART
NATIONAL BUREAU OF STANDARDS-1963-A

18 DNA 4184F
SBIE
19 AD-E300118

BASIC REQUIREMENTS FOR NUCLEAR TESTING OF A HEAT-SINK CONCEPT

R & D Associates
P.O. Box 9695
Marina del Rey, California 90291

12

11 October 1974

12 44 p.

9 Final Report for Period July 1974—October 1974

14 CONTRACT No. DNA 001-74-C-0139

RDA-TR-5900-012

15

10 J. E. Whitener

16 P99QAXD

17 B00L

THIS WORK SPONSORED BY THE DEFENSE NUCLEAR AGENCY
UNDER RDT&E RMSS CODE B310075464 P99QAXDB00113 H2590D.

Prepared for
Director
DEFENSE NUCLEAR AGENCY
Washington, D. C. 20305

390 124

Destroy this report when it is no longer needed. Do not return to sender.

UNCLASSIFIED

SECURITY CLASSIFICATION OF THIS PAGE *(When Data Entered)*

REPORT DOCUMENTATION PAGE		READ INSTRUCTIONS BEFORE COMPLETING FORM
1. REPORT NUMBER DNA 4184F	2. GOVT ACCESSION NO.	3. RECIPIENT'S CATALOG NUMBER
4. TITLE *(and Subtitle)* BASIC REQUIREMENTS FOR NUCLEAR TESTING OF A HEAT-SINK CONCEPT		5. TYPE OF REPORT & PERIOD COVERED Final Report for Period Jul 74—Oct 74 6. PERFORMING ORG. REPORT NUMBER RDA-TR-5900-012
7. AUTHOR(s) J. E. Whitener		8. CONTRACT OR GRANT NUMBER(s) DNA 001-74-C-0139
9. PERFORMING ORGANIZATION NAME AND ADDRESS R&D Associates P.O. Box 9695 Marina Del Rey, California 90291		10. PROGRAM ELEMENT, PROJECT, TASK AREA & WORK UNIT NUMBERS Subtask P99QAXDB001-13
11. CONTROLLING OFFICE NAME AND ADDRESS Director Defense Nuclear Agency Washington, D.C. 20305		12. REPORT DATE October 1974 13. NUMBER OF PAGES 46
14. MONITORING AGENCY NAME & ADDRESS*(if different from Controlling Office)*		15. SECURITY CLASS *(of this report)* UNCLASSIFIED 15a. DECLASSIFICATION/DOWNGRADING SCHEDULE

16. DISTRIBUTION STATEMENT *(of this Report)*

Approved for public release; distribution unlimited.

17. DISTRIBUTION STATEMENT *(of the abstract entered in Block 20, if different from Report)*

18. SUPPLEMENTARY NOTES

This work sponsored by the Defense Nuclear Agency under RDT&E RMSS Code B310075464 P99QAXDB00113 H2590D.

19. KEY WORDS *(Continue on reverse side if necessary and identify by block number)*

Carbon Heat Sink
Seismic Decoupling
Cavity Pressure
Displacement Potential
Scaling Relations
HE versus Nuclear

20. ABSTRACT *(Continue on reverse side if necessary and identify by block number)*

This report was prepared as a part of the PRE-MINE DUST test program, funded by ARPA and monitored by DNA. The basic objective of the work is to provide guidelines for a nuclear test of a heat-sink concept for reducing the size of a cavity required for seismic decoupling of underground nuclear explosions. The concept is also of interest in engineering the containment of explosions.

DD FORM 1 JAN 73 1473 EDITION OF 1 NOV 65 IS OBSOLETE

UNCLASSIFIED

SECURITY CLASSIFICATION OF THIS PAGE *(When Data Entered)*

PREFACE

The objectives of this report are (1) to review the development of a heat-sink concept in order to minimize the cavity size necessary to quench an underground nuclear explosion; and (2) to provide the basic requirements for a test to verify the technique.

This report was prepared as a part of the PRE-MINE DUST test program sponsored by the Advanced Research Proejcts Agency and monitored by the Defense Nuclear Agency.

The results of this study are expected to provide an input to ARPA's nuclear monitoring programs and to assist DNA in efforts to engineer the containment of underground nuclear explosions.

Conversion factors for U.S. customary to metric (SI) units of measurement.

To Convert From	To	Multiply By
angstrom	meters (m)	1.000 000 X E -10
atmosphere (normal)	kilo pascal (kPa)	1.013 25 X E +2
bar	kilo pascal (kPa)	1.000 000 X E +2
barn	meter^2 (m^2)	1.000 000 X E -28
British thermal unit (thermochemical)	joule (J)	1.054 350 X E +3
calorie (thermochemical)	joule (J)	4.184 000
cal (thermochemical)/cm^2	mega joule/m^2 (MJ/m^2)	4.184 000 X E -2
curie	*giga becquerel (GBq)	3.700 000 X E +1
degree (angle)	radian (rad)	1.745 329 X E -2
degree Fahrenheit	degree kelvin (K)	$t_K = (t°f + 459.67)/1.8$
electron volt	joule (J)	1.602 19 X E -19
erg	joule (J)	1.000 000 X E -7
erg/second	watt (W)	1.000 000 X E -7
foot	meter (m)	3.048 000 X E -1
foot-pound-force	joule (J)	1.355 818
gallon (U.S. liquid)	meter^3 (m^3)	3.785 412 X E -3
inch	meter (m)	2.540 000 X E -2
jerk	joule (J)	1.000 000 X E +9
joule/kilogram (J/kg) (radiation dose absorbed)	Gray (Gy)	1.000 000
kilotons	terajoules	4.183
kip (1000 lbf)	newton (N)	4.448 222 X E +3
kip/inch^2 (ksi)	kilo pascal (kPa)	6.894 757 X E +3
ktap	newton-second/m^2 ($N-s/m^2$)	1.000 000 X E +2
micron	meter (m)	1 000 000 X E -6
mil	meter (m)	2.540 000 X E -5
mile (international)	meter (m)	1.609 344 X E +3
ounce	kilogram (kg)	2.834 952 X E -2
pound-force (lbs avoirdupois)	newton (N)	4.448 222
pound-force inch	newton-meter (N·m)	1.129 848 X E -1
pound-force/inch	newton/meter (N/m)	1.751 268 X E +2
pound-force/foot^2	kilo pascal (kPa)	4.788 026 X E -2
pound-force/inch^2 (psi)	kilo pascal (kPa)	6.894 757
pound-mass (lbm avoirdupois)	kilogram (kg)	4.535 924 X E -1
pound-mass-foot^2 (moment of inertia)	kilogram-meter^2 ($kg·m^2$)	4.214 011 X E -2
pound-mass/foot^3	kilogram/meter^3 (kg/m^3)	1.601 846 X E +1
rad (radiation dose absorbed)	**Gray (Gy)	1.000 000 X E -2
roentgen	coulomb/kilogram (C/kg)	2.579 760 X E -4
shake	second (s)	1.000 000 X E -8
slug	kilogram (kg)	1.459 390 X E +1
torr (mm Hg, 0° C)	kilo pascal (kPa)	1.333 22 X E -1

*The becquerel (Bq) is the SI unit of radioactivity; 1 Bq = 1 event/s.
**The Gray (Gy) is the SI unit of absorbed radiation.

A more complete listing of conversions may be found in "Metric Practice Guide E 380-74," American Society for Testing and Materials.

TABLE OF CONTENTS

Section		Page
1	INTRODUCTION	7
	1.1 DIAMOND DUST Concept	7
	1.2 Void Space Configuration	7
	1.2.1 Graphite-Filled Chamber	9
	1.2.2 Graphite Powder Plus Air Cells	9
	1.2.3 Coke	9
	1.2.4 Parametric Variations	9
	1.3 PRE-MINE DUST	10
	1.3.1 Chamber Pressure	12
	1.3.2 High-Speed Photography	12
	1.3.3 Impulse on Chamber Wall	12
	1.3.4 Time-of-Arrival	14
	1.3.5 Decoupling Measurements	14
	1.4 Summary of HE Tests	16
2	NUCLEAR VERSUS HIGH EXPLOSIVE ENERGY QUENCHING	17
	2.1 Comparison of Heat Sinks	17
	2.2 Other Qualitative Differences	18
	2.2.1 Source Temperature Effects	18
	2.2.2 Contaminants	19
	2.3 Equation-of-State of Carbon	20
	2.4 Application of the Equation-of-State	23
3	NUMERICAL CALCULATIONS	26
	3.1 Simulated Heat-Sink Calculation	26
	3.2 Tamped Burst Calculation	26
	3.3 Comparison of Results	26
	3.4 Comments on the Numerical Results	29
4	SPECIFICATIONS FOR A NUCLEAR TEST	31
	4.1 Nuclear Yield	31
	4.1.1 Seismic Source	31
	4.1.2 X-Ray Energy	32
	4.2 Carbon Heat-Sink Configuration	32
	4.2.1 Cavity Size	32
	4.2.2 Sources of Carbon	33
	4.2.3 Forming Void Space	33
	4.2.4 Coke Chunks	34
	4.2.5 Balloons	34
	4.2.6 Suspension Support	36

TABLE OF CONTENTS (CONT.)

Section		Page
4.3	Summary of Basic Design Specifications	38
4.4	Basic Measurements	39
4.4.1	Seismic Measurements	39
4.4.2	Close-In Ground Motion	39
4.4.3	Cavity Pressure versus Time	39
4.4.4	Close-In Ground Stress Measurements	39
4.5	Numerical Support Calculations	39
4.6	Ground Medium for Decoupling	40
	REFERENCES	41

LIST OF ILLUSTRATIONS

Figure		Page
1	Comparison of Initial Cavity Size for Fully Decoupled Cavity and Cavities with Heat Sinks - - - - - - - - - - - - - - - - - -	8
2	Average Measured vs. Calculated Impulse from Strong Shock Theory - - - - - - - - - - -	13
3	Comparison of Measured Time-of-Arrival vs. Calculation from Strong Shock Theory -	15
4	Carbon Vapor Pressure vs. Temperature in Two-Phase Equilibrium - - - - - - - - - - -	21
5	Carbon Vapor Pressure vs. Density in Two-Phase Equilibrium - - - - - - - - - - - -	22
6	Relationship Between Carbon Vapor Pressure, Carbon Density, and Cavity Volume - - - - -	24
7	Ground Radial Stress and Displacement - - -	27
8	Ground Radial Stress and Displacement - - -	28
9	Schematic Illustration of Heat-Sink - - - -	37

LIST OF TABLES

Table		Page
1	Variation of Bubble Size - - - - - - - - - - -	11
2	Coke Experiments in Air Medium - - - - - - - -	11
3	Comparison of Displacement and Volume Displaced - - - - - - - - - - - - - - - - - - -	29

SECTION 1. INTRODUCTION

The radius of an air-filled cavity in hard rock required to decouple an underground nuclear explosion has been previously estimated to be about 25 meters $W^{1/3}$ (KT). For yields of 10 KT and larger, the cavity size appears prohibitively large to mine in hard rock, both for economic and perhaps construction reasons. As a result, several test programs and theoretical effort have been conducted to investigate the use of heat absorbers to reduce the cavity size required. The principal problems associated with a heat absorber technique are in achieving adequate and rapid mixing of the explosive gases and the absorber material.

The DIAMOND DUST, DIAMOND MINE and PRE-MINE DUST test programs to study heat absorber concepts for quenching an explosion in a cavity are summarized in References 1, 2, 3 and in the included reference lists.

1.1 DIAMOND DUST CONCEPT

DIAMOND DUST was a test of use of a heat sink to absorb the energy of a nuclear explosion in a cavity. Graphite powder was placed around the explosive source, and measurements were made to determine the effectiveness of the heat-sink concept. Figure 1 illustrates the reduction in volume achieved in the DIAMOND DUST concept compared to that in an air-filled cavity. DIAMOND DUST was conservatively planned, with a cavity probably larger than necessary.

1.2 VOID SPACE CONFIGURATION

Following the DIAMOND DUST test, additional HE experiments were conducted in a small 1-ft-diameter pressure chamber to study other heat-sink configurations [4]. In particular, by increasing the mass of carbon, the cavity volume could be

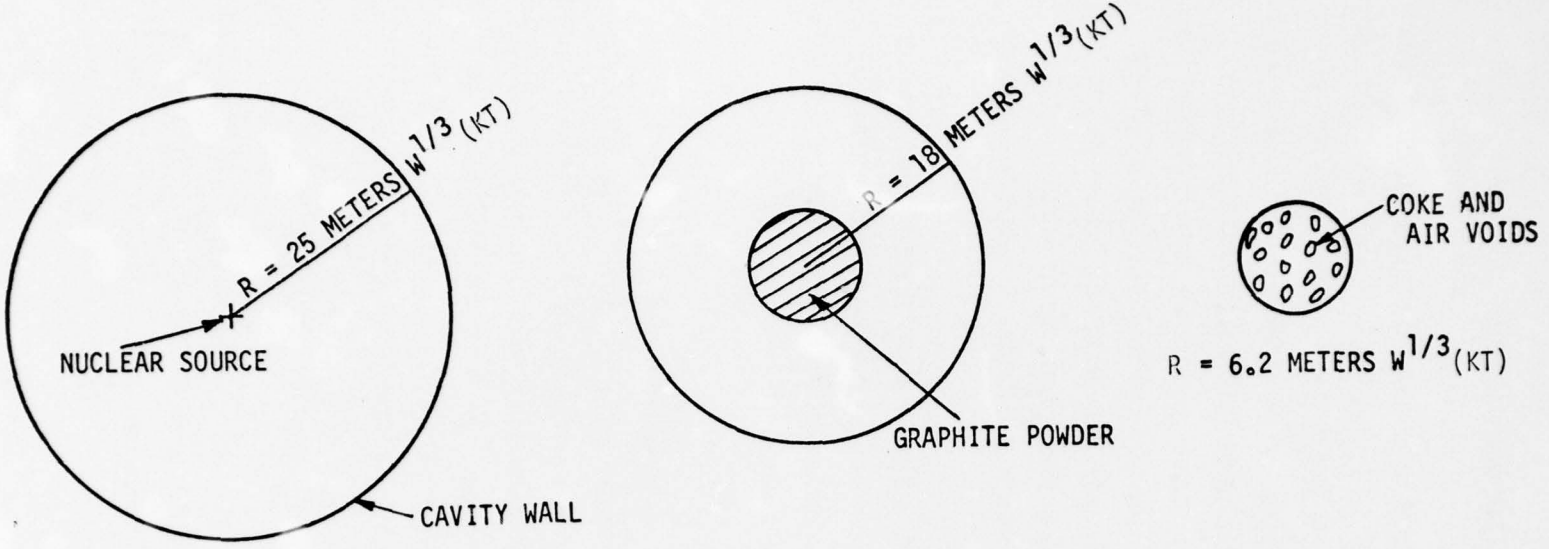

VOLUME = 6.5×10^4 m^3W(KT)
AIR-FILLED CAVITY

VOLUME = 2.4×10^4 m^3W(KT)
DIAMOND DUST CONCEPT

VOLUME = 1000 m^3W(KT)
PRE-MINE DUST CONCEPT

Figure 1. Comparison of Initial Cavity Size for Fully Decoupled Cavity and Cavities with Heat Sinks

reduced if proper quenching occurred. Whereas on DIAMOND DUST, about 0.5 kiloton of carbon per-kiloton of yield was used, the mass of carbon was increased in these experiments to about 16 or more kilotons of carbon per kiloton of HE--a factor of 32 or greater.

1.2.1 Graphite-Filled Chamber

The chamber was filled with fine graphite powder, with a natural bulking density of 0.5 gm/cm^3, surrounding a 0.5-lb HE charge. Results showed that the pressure was considerably reduced but higher than predicted. Compaction of the graphite at the chamber wall further indicated that proper mixing had not occurred.

1.2.2 Graphite Powder Plus Air Cells

In an attempt to improve the mixing, plastic air cells were dispersed throughout the graphite powder so as to provide passageways for the HE gases to penetrate the carbon. The test was successful in producing the calculated equilibrium pressure.

1.2.3 Coke

A third modification of the heat-sink configuration was tested, where coke chunks were used in place of the graphite powder [5]. Bulking of the coke chunks provided about equal air-void and solid space which would eliminate the need for the air cells. In addition, the yield strength of the coke was quite small, allowing pulverization by the high pressures produced.

1.2.4 Parametric Variations

Incomplete mixing in the first set of experiments discussed above suggested that the size of the air-voids was an important parameter in the mixing process. A parametric variation of the air-void size was made on several shots using various

sizes of air cells and different sizes of coke chunks in the graphite powder. Tables 1 and 2 show qualitatively that voids too small reduced the mixing, as indicated by measured chamber pressures higher than predicted.

The results of the 1-ft chamber experiments verified that a much larger carbon/HE weight-ratio, compared to DIAMOND DUST, would result in satisfactory quenching provided air-void spaces were sufficiently large. This was quite significant since the successful application to tests involving nuclear yields could greatly reduce the cavity volume as indicated in Figure 1. However, the credibility of applying the modified quenching technique to kilotons of yield--more than six orders of magnitude greater--was highly uncertain. Additional HE tests using much larger yields than the previous ones might be expected to provide some guidelines for scaling to nuclear tests of interest.

The PRE-MINE DUST test program was planned and executed to extend the HE testing of the heat-sink concept to nearly 2000 times larger yield than in the 1-ft chamber tests.

1.3 PRE-MINE DUST

The principal experiments to investigate effects of increased yield on quenching are outlined in the subsections that follow. Experiments similar to those discussed under Subsection 1.2 were conducted in the following configurations:

- 1-ft-diameter chamber with 0.5 lb HE.
- 6-ft-diameter chamber with 100 lb HE.
- 12-ft-diameter cavity in tuff with 1000 lb HE, an overall span of about 2000 in yield and volume.

Table 1. Variation of Bubble Size

(Bubble fraction $\simeq$ 1/2, HE charge = 250 gm, graphite = 4000 gm, bulk density of graphite $\simeq$ 1/2)

Experiment Number	Bubble Size (in)	Calculated Pressure for Complete Mixing (psi)	Measured Pressure (psi)	Calculated Pressure if no Heat Transfer (psi)
A-1674	0	594	1025	3900
A-1604	3/8	594	600	3900
A-1598	1	594	600	3900
A-1668	3-1/4	594	610	3900

Table 2. Coke Experiments in Air Medium

(Density of coke $\simeq$ 1 gm/cm^3, void fraction $\simeq$ 1/2)

Coke Size (in)	Coke Mass (gm)	HE Charge (gm)	Calculated Pressure for Complete Mixing (psi)	Measured Pressure (psi)	Calculated Pressure if no Heat Transfer (psi)
1/4	6770	250	525	850	4400
1/4	7500	250	600	850	4500
1	7000	250	605	650	4400
1	7000	250	605	660	4400
1	6665	500	1440	1660	8700
3	7000	250	605	725*	4400
3	6995	250	605	700*	4400

*At 40 ms: measured pressure = 600 psi.

1.3.1 Chamber Pressure

Results showed that the equilibrium chamber pressure was consistent with calculations over the yield range tested. It was also observed in the 6-ft chamber tests that complete mixing did not occur when the sizes of the coke chunks (or the air-void spaces) were too small. Compaction of the carbon was also observed at the cavity wall in these cases.

1.3.2 High-Speed Photography

Motion picture photography was used to observe the penetration of hot HE products through coke surrounding the HE charge. Several shots were fired with various sizes of coke chunks and total mass of the coke.

Results confirmed that when the mass of coke was increased, the coke size must also be increased for gas penetration to occur.

1.3.3 Impulse on Chamber Wall

The dynamic impulse on the wall due to carbon impact was observed on all the shots. Despite penetration of the gases through the voids, sufficient drag forces resulted in motion of the carbon to produce a large pressure spike. The concern over the impulse is the effect on seismic decoupling. Even though quenching (reduction of cavity pressure) occurs, inelastic motion at the cavity wall, due to the pressure spike, might degrade decoupling efficiency.

Impulse measurements were made and compared to calculated values using the strong-shock theory of explosions in gases. Figure 2 shows the average value of measurements at each HE charge size versus the calculated values. Bounds are shown for complete inelastic and elastic impacts. These results are expected to be useful in estimating (within a factor of two) the impulse resulting from arbitrary yield, cavity size, and mass of carbon.

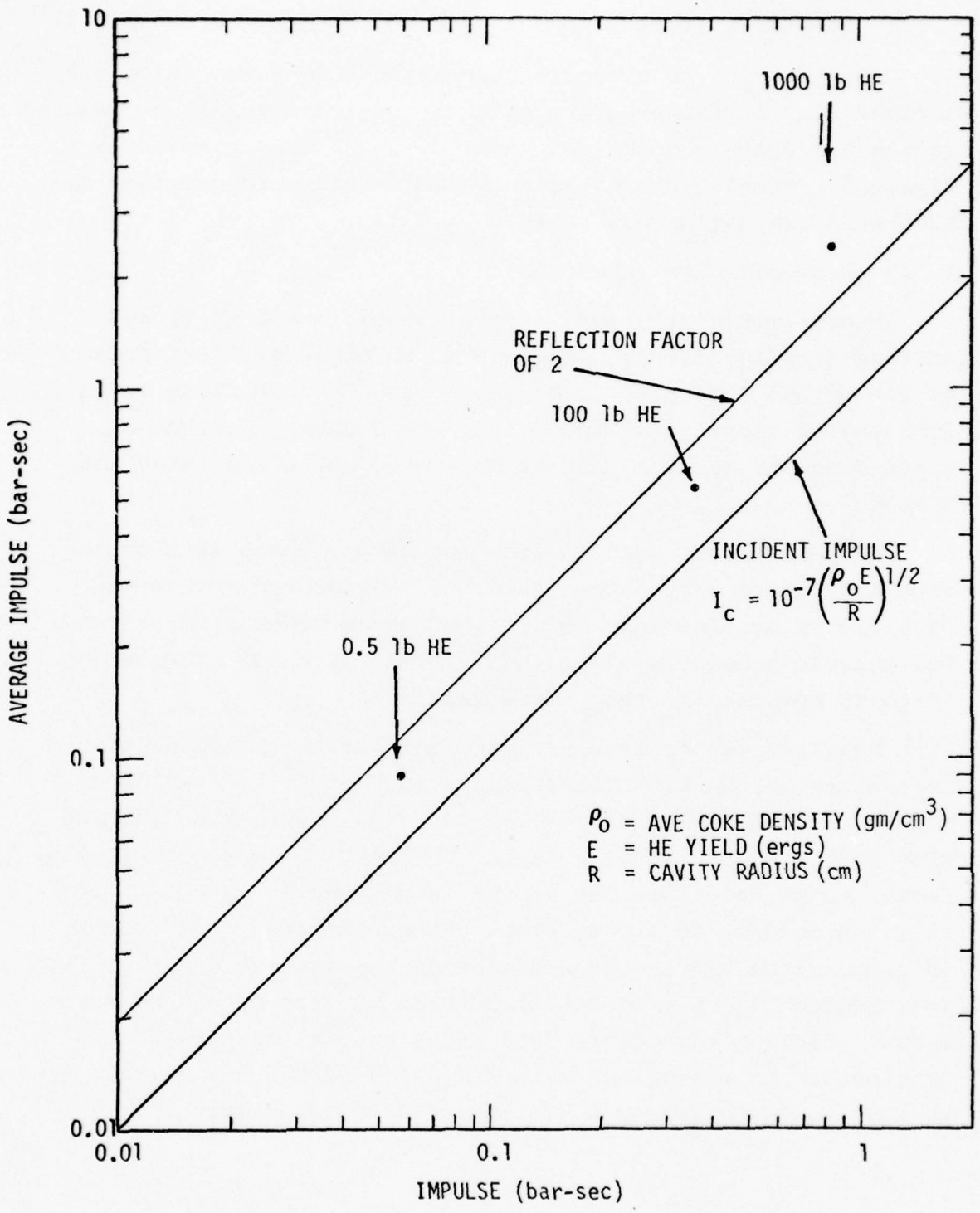

Figure 2. Average Measured vs. Calculated Impulse from Strong Shock Theory

1.3.4 Time-of-Arrival

Another clue to a scaling law was the measurement of the arrival time of the pressure spike at the cavity wall. Measured values are again compared with strong shock theory as shown in Figure 3. Results shown are for all measurements covering the HE charge range from 0.5 to 1000 lb.

1.3.5 Decoupling Measurements

Measurements of ground stress, particle velocity, and surface-seismic signals were made on three 1000-lb HE shots at the Nevada Test Site to estimate seismic decoupling resulting from cavity quenching. Two of the three shots occurred in 12-ft-diameter cavities containing coke, while the third was tamped.

Comparisons of results from the cavity shots with those from the tamped shot showed that the peak ground stress and particle velocities were lower by about an order of magnitude. The seismic signal levels were also less by about a factor of 10 to 20 compared to the tamped case.

Previous estimates have been made for the maximum seismic decoupling for an air-filled cavity in tuff [6]. A value of 40 was obtained as compared with 10 to 20 observed on the PRE-MINE DUST results. This apparent degradation in the decoupling factor might have been due to the large impulse at the cavity wall. According to strong shock theory in gases, the impulse is proportional to the square-root of the ambient density (see Figure 2). The agreement between the theory and measurements, treating the carbon as a heavy gas, shows that the impulse due to the carbon with a density of 0.5 gm/cm^3, compared to air, would be larger by $(0.5/0.0013)^{1/2}$ or nearly 20.

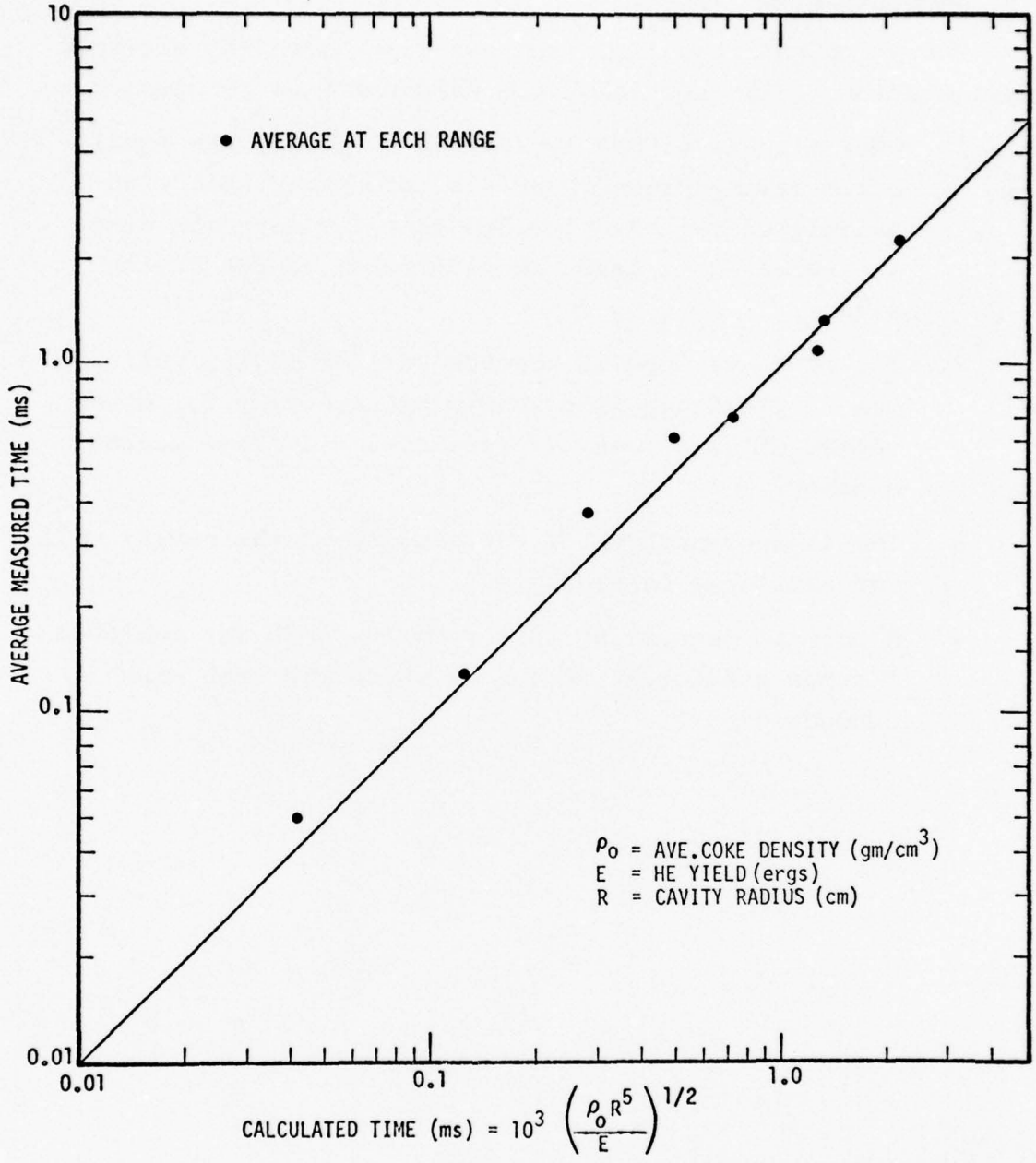

Figure 3. Comparison of Measured Time-of-Arrival vs. Calculation from Strong Shock Theory

1.4 SUMMARY OF HE TESTS

The principal results of the experiments on the air-void configuration of the heat-sink are summarized as follows:

1. Over a range of nearly 2000 in HE yield, the equilibrium cavity pressure agrees reasonably well with calculated values, provided that the air-void size is increased at least in proportion to the cavity size.
2. The pressure impulse produced at the cavity wall can be predicted with sufficient accuracy for given values of yield, cavity radius, and average carbon density.
3. The time-of-arrival of the impulse at the cavity wall can similarly be predicted.
4. A seismic decoupling factor of 10 to 20 was achieved for the particular medium in which the test was conducted.

SECTION 2. NUCLEAR VERSUS HIGH EXPLOSIVE ENERGY QUENCHING

The PRE-MINE DUST HE test program has demonstrated that satisfactory quenching occurs when carbon, surrounding an HE charge, is permeated with air-void spaces which are sufficiently large. Furthermore, the technique was successful covering a range of nearly 2000 in yield. Since the largest HE charge was 0.5 tons, another increase in yield by a factor of 2000 is needed to extrapolate results to a kiloton HE test. In order to illustrate the difference between quenching HE and a nuclear explosion, a comparison is made based upon the same yield and same equilibrium cavity pressure.

2.1 COMPARISON OF HEAT SINKS

The basis for comparison will be to assume an equilibrium cavity pressure of 100 bars for both cases. An average density of 0.5 gm/cm^3 of coke is assumed. Previous test results have shown that this value is about optimum for minimum cavity volume and allowing for 50 percent void spaces. A yield of 1 KT is assumed.

The calculated values of the design parameters are shown for comparison.

	Nuclear	HE
Energy	1 KT	1 KT
Cavity pressure	100 bars	100 bars
Carbon density	0.5 gm/cm^3	0.5 gm/cm^3
Cavity volume	1000 m^3	2.2×10^4 m^3
Cavity radius	6.2 m	18 m
Charge radius	--	5.8 m
Carbon weight	0.6 kt	12 kt
Carbon and gas temperature	$\sim$4000° K	600° K
Carbon heat content	2000 cal/gm	80 cal/gm

The greater size of the HE configuration is principally due to the lower energy density of the high explosive. The mass of air and carbon vapor in the nuclear case is small compared to that of the high explosive products. At the conditions chosen, the heat content of the carbon in the HE case is only 80 cal/gm, as compared to 2000 cal/gm in the nuclear heat sink. This accounts for the much larger mass of carbon and cavity volume needed to quench a high-explosive source.

The PRE-MINE DUST experiments discussed have shown that scaling can be applied to heat-sink tests as long as HE sources are considered. However, a comparison of nuclear versus HE quenching, discussed in Section 2, shows that scaling from low-yield HE test results would not apply to a nuclear source of the same yield. Cavity volume, carbon mass, and void space do not scale properly from HE to nuclear sources.

2.2 OTHER QUALITATIVE DIFFERENCES

2.2.1 Source Temperature Effects

As a consequence of the higher energy density of a nuclear source, the temperature may result in release of a large fraction of the energy in thermal radiation which is negligible in the case of high explosives. Vaporization of carbon close-in by radiation absorption might affect in some way the overall mixing process.

Another temperature effect which seems plausible is that the particle velocity of the debris gases is much greater than that from an HE explosion. It might be expected that the process of mixing of the hot debris gases with the carbon would be enhanced.

A smaller mass of gas than that produced by HE might impart less momentum and velocity to the carbon allowing

more of the gases to penetrate through the voids before choking, due to snowplowing of the carbon, could occur.

2.2.2 Contaminants

An important consideration in the application of the carbon heat-sink concept of nuclear tests is that of the carbon purity. At the equilibrium temperature (4000° K or greater), most impurities, such as water, sulphur, and ash will vaporize, increasing the total equilibrium pressure in the cavity. At temperature equilibrium using high explosives, most impurities in the carbon will not volatilize at the low temperature. A greater cavity pressure would increase the ground displacement; hence, the decoupling would be reduced.

To illustrate how an impurity in the carbon would increase the cavity pressure, water is chosen as an example. The pressure is calculated from the ideal gas law

$$PV = nRT$$

where V = cavity volume

m = mass of carbon

f = fraction of H_2O

T = equilibrium temperature

n = number of moles of H_2O

M = molecular weight of H_2O (4000° K).

Then

$$P = \frac{fm}{M} \cdot \frac{RT}{V} .$$

Using the values shown for the nuclear case in Subsection 2.1 and the equation-of-state for water from Reference 7, the calculated pressure is

$$P_{bars} = 1.3 \times 10^4 f.$$

This result shows, for example, that only 1 percent of water would produce 130 bars pressure.

It is difficult to assess the relative importance of this effect since the impulse on the cavity wall, due to the carbon, will also increase the permanent displacement.

2.3 EQUATION-OF-STATE OF CARBON

Another important difference in the quenching of nuclear versus HE explosions using carbon is the different temperature regimes of the equation-of-state. Whereas a temperature rise of only about 150 to 200° C occurred in the HE experiments, temperatures in the neighborhood of 4000° C would be expected in the case of quenching a nuclear explosion. The amount of carbon vaporized by HE is negligible; while in the nuclear case, the main contribution to the cavity pressure is expected to be carbon vapor.

The heat capacity of carbon at the low temperature in the HE experiments has been accurately determined experimentally. Vapor pressure of carbon is negligible compared to that of the HE products. Most of the energy is absorbed by heat conduction into solid carbon.

Equilibrium conditions for nuclear quenching, however, are more uncertain at high temperature due to the lack of experimental verification of the theoretical equation-of-state of carbon.

To illustrate the current status of the equation-of-state of carbon in the temperature range of interest, Figures 4 and 5 are plots of the vapor pressure versus temperature and vapor density respectively. The vapor is in equilibrium with the solid phase. Curves are shown for calculations obtained from

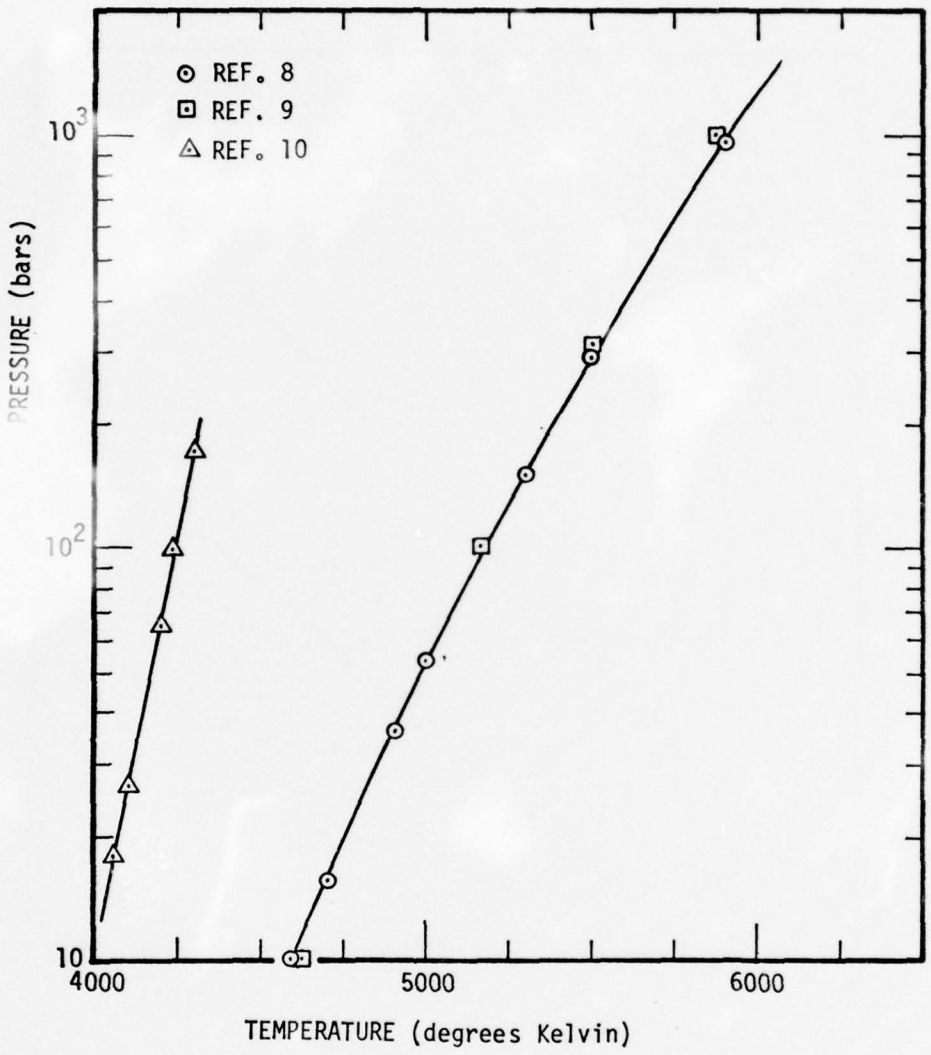

Figure 4. Carbon Vapor Pressure vs. Temperature in Two-Phase Equilibrium

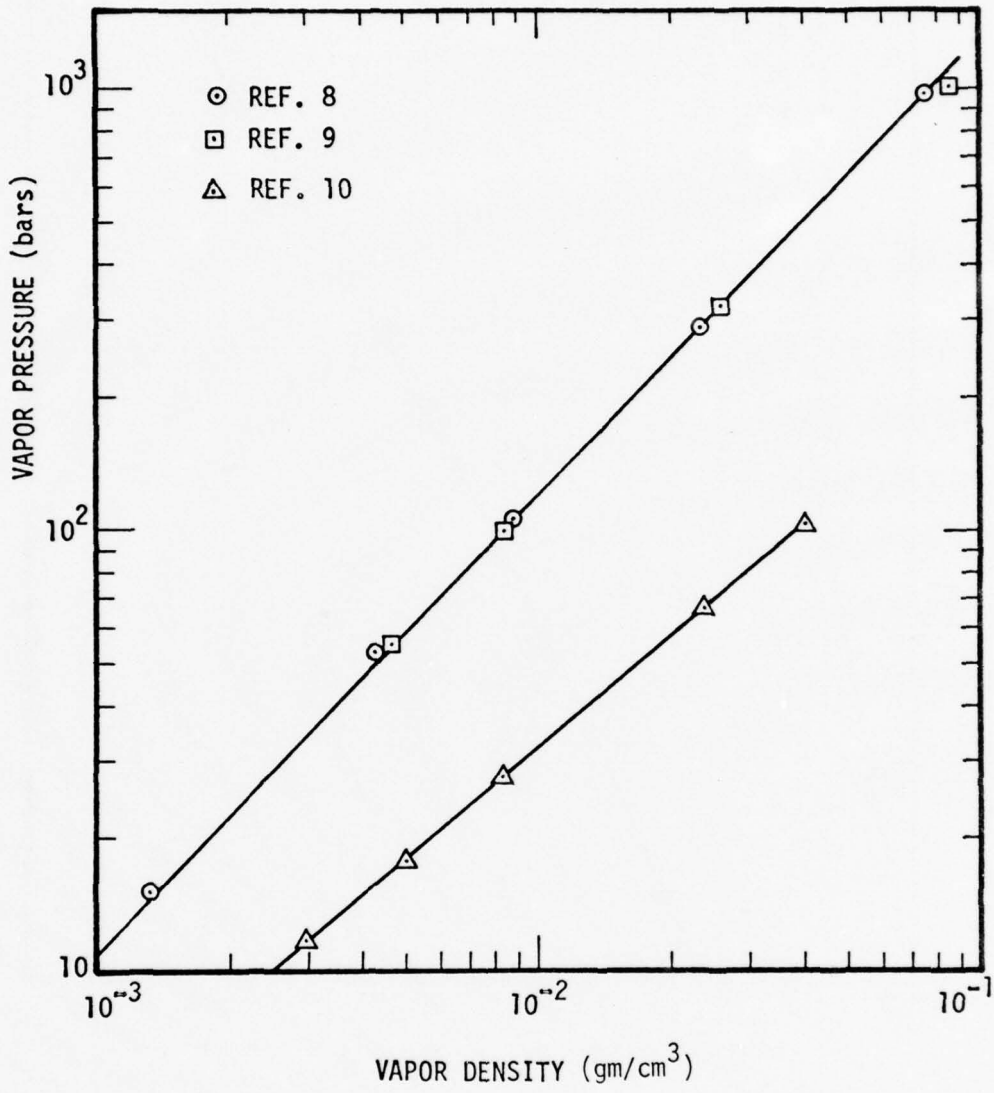

Figure 5. Carbon Vapor Pressure vs. Density in Two-Phase Equilibrium

References 8, 9, and 10. The main differences in the calculations were the number of molecular species chosen for the vapor phase of carbon. In References 8 and 9, the species assumed were C_1 through C_5 and C_1 through C_{12} respectively, while C_1 through C_{30} were used in the calculations of Reference 10. Also in Reference 10, some experimental data on the triple-point were included. Along with several other assumptions involved in the calculations, the uncertainty in the equation-of-state of carbon is probably represented by the differences in the results shown. Among other expertise on the high temperature equation-of-state of carbon, it is generally agreed that because of the difficulty in obtaining experimental data at high temperature, a considerable degree of uncertainty exists.

2.4 APPLICATION OF THE EQUATION-OF-STATE

In this report, emphasis is placed on minimization of the cavity volume in order to reduce mining costs and engineering problems associated with the construction of large cavities. However, as the cavity size is reduced, the mass of carbon required for a prescribed cavity pressure must be increased in order to maintain the corresponding temperature. There is a limit to which this approach can be pushed, since as the cavity size is reduced, the carbon density would be increased such that in the final limit, no void space would be available for mixing of the hot debris gases with the carbon. Hence, a tamped explosion would result with no cavity decoupling. Experience with various forms of carbon used in the HE tests shows that the average density, resulting from natural bulking of irregular shaped chunks, lies between 0.25 and 1.0 gm/cm^3.

From References 8, 9, and 10, a graph is constructed in Figure 6 to provide a basis for the heat-sink design. The

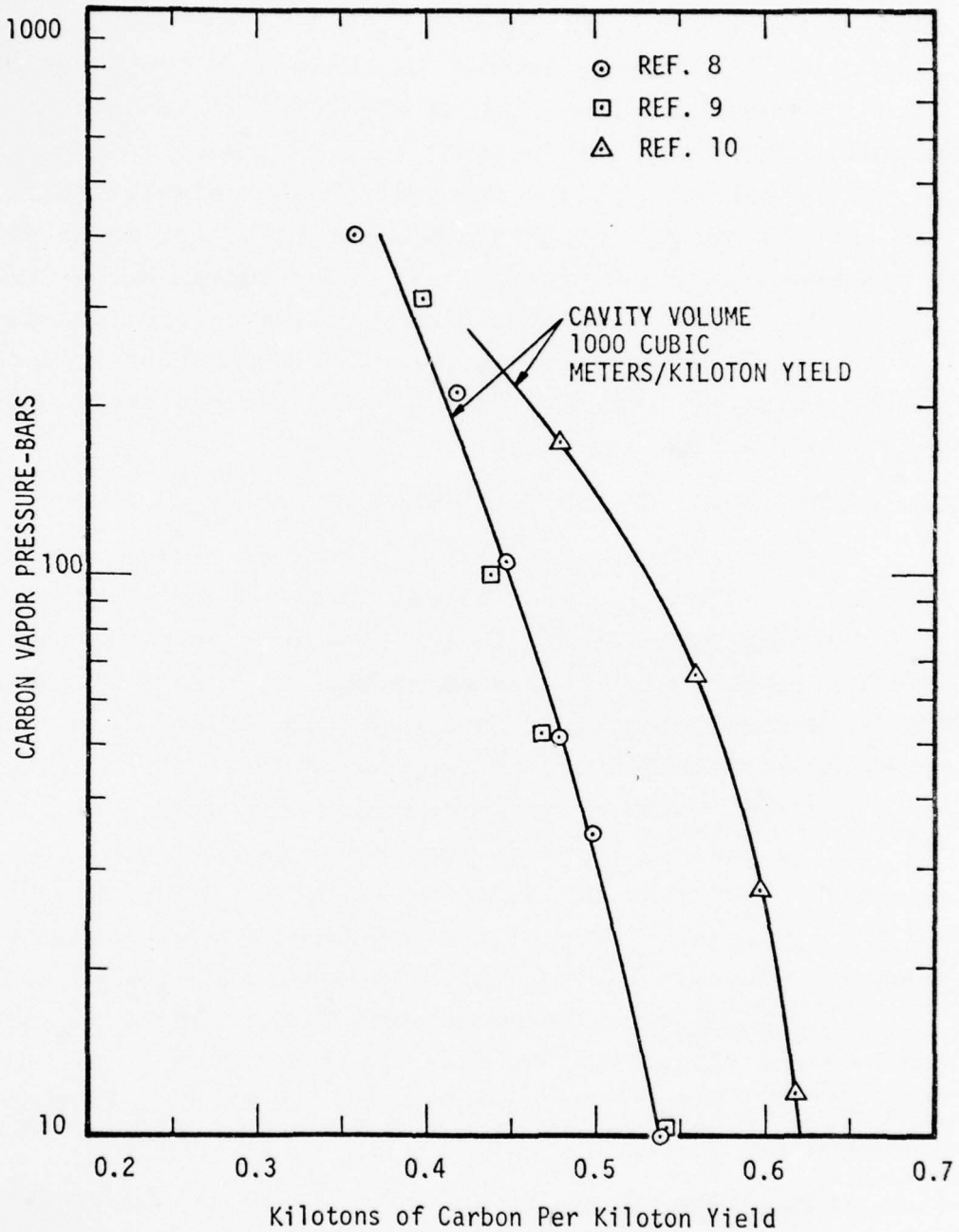

Figure 6. Relationship Between Carbon Vapor Pressure, Carbon Density, and Cavity Volume

two curves again show the uncertainty in the equation-of-state of carbon. However, above a pressure of 200 bars, the curves appear to merge.

Vapor pressure of carbon is plotted against the mass of carbon required for a given yield and cavity volume. Moving along a given curve shows the dependence of vapor pressure upon the mass of carbon for a given cavity volume. The steepness of the curves is due to the strong dependence of vapor pressure upon temperature in two-phase equilibrium. The scale for the carbon mass is also approximately the carbon density in grams/cubic centimeter.

Figure 6 generally covers the region of the equation-of-state for carbon to be used in the design of a heat sink that would minimize the cavity volume required for quenching.

SECTION 3. NUMERICAL CALCULATIONS

In order to estimate the seismic decoupling which might be achieved by using the heat-sink model in a nuclear test, some numerical calculations were made. A comparison of the near-in ground motions, produced by an explosion in a cavity using a heat sink with those motions produced by a tamped burst, was used to estimate the decoupling.

3.1 SIMULATED HEAT-SINK CALCULATION

Numerical calculations of the mixing and energy absorption phase of quenching were not included in this calculation. Instead, results from a previous calculation [11] were used to begin the problem when the shock arrived at the cavity wall. That calculation was made for a 1-KT explosion at the center of a cavity filled with 0.5 gm/cm^3 of carbon. Impulse and pressure on the cavity wall were then applied as inputs for the present calculation to determine the ground motion in tuff [12].

3.2 TAMPED BURST CALCULATION

This computation was also performed for 1-KT yield in tuff. Both calculations were carried to a distance where the ground motion became elastic.

3.3 COMPARISON OF RESULTS

Results from the two calculations of ground-particle displacement and radial stress are shown in Figures 7 and 8 for the quenched and tamped cases respectively. The comparisons are made at ranges where the peak stresses are approximately equal.

Of particular interest here is the comparison of the final displacements and distances from the burst points. The relative decoupling factor, which is the ratio of the seismic strengths for two explosions, is estimated by

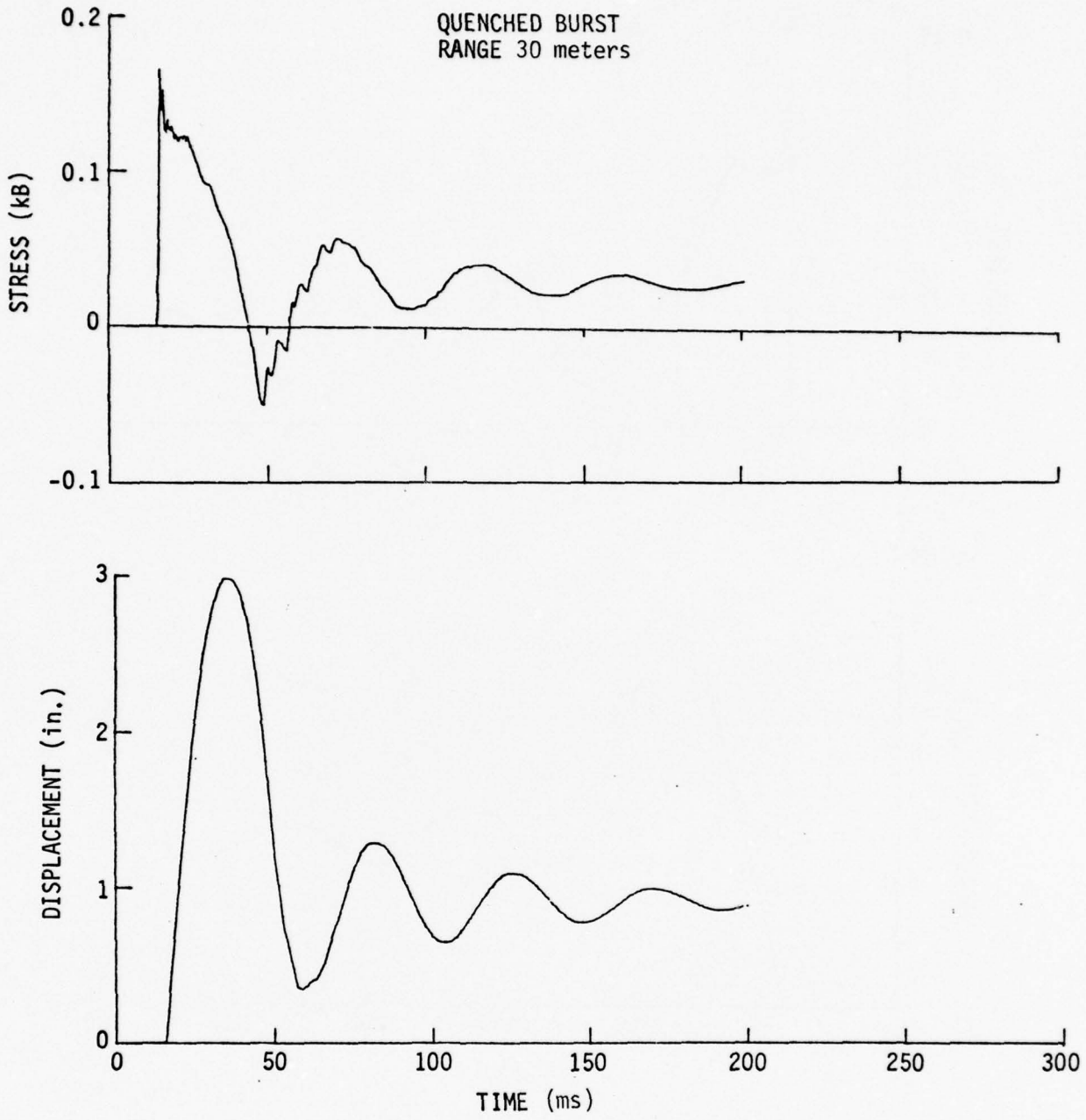

Figure 7. Ground Radial Stress and Displacement

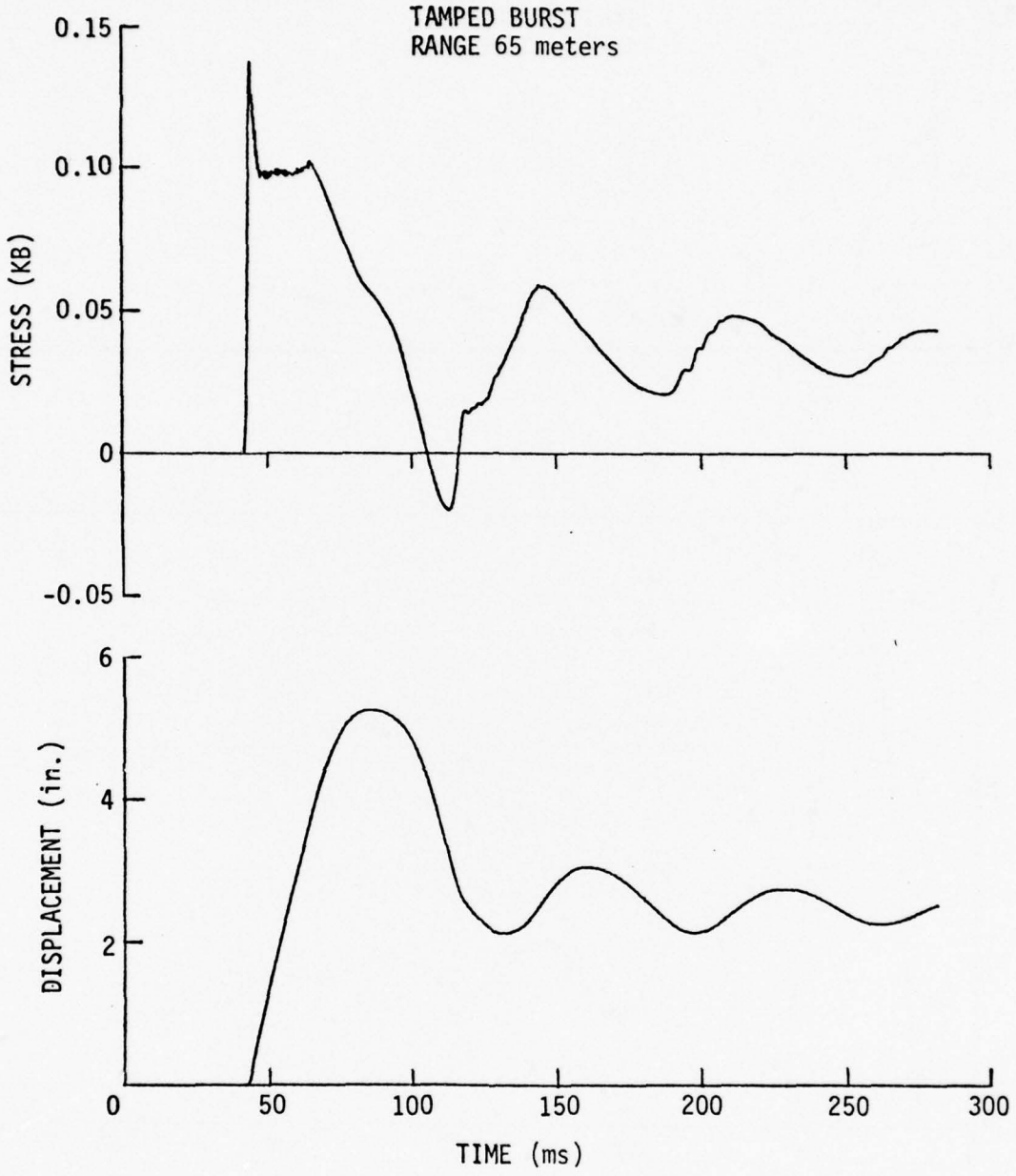

Figure 8. Ground Radial Stress and Displacement

$$\text{Decoupling factor} = \frac{(R^2 d)\ \text{tamped}}{(R^2 d)\ \text{cavity}}$$

where R = range and d = permanent displacement. The quantity $R^2 d$ is proportional to the volume displaced at a given range.

From the two figures, it is noted that the final displacement for the tamped burst is larger by almost a factor of three at a distance more than twice as great. Table 3 summarizes the pertinent results.

The tamped/cavity ratio of $R^2 d$ shows a decoupling of about 14. This result is comparable to results obtained from seismic measurements made on the PRE-MINE DUST HE tests.

3.4 COMMENTS ON THE NUMERICAL RESULTS

It is important to point out that several assumptions, used in the calculations, were made in formulating the constitutive relations describing the elastic-plastic behavior of the rock medium during loading and unloading. In particular, uncertainty of the yield-failure criteria, porosity, and water content can result in a wide variation in the calculated ground motions.

Some results of the tamped calculations discussed above can be compared to measurements of ground particle displacement on the Ranier event [13]. Ranier was the first nuclear test

Table 3. Comparison of Displacement and Volume Displaced

Shot	Distance (meters)	Final Disp (cm)	$R^2 d$ (m^3)
Tamped	65	6.6	278
Cavity	30	2.3	20.4

to establish a data base used to estimate the decoupling factor for an explosion in a cavity.

A comparison of the peak displacements shows that the experimental results are about 50 percent greater than the calculated values. Also the high frequency amplitudes are lower by about a factor of two. This result indicates that the calculations are probably correct within the same order.

Results of the cavity calculation showed that the dynamic impulse, delivered to the cavity wall by the carbon impact, produced a large displacement of the wall. A reduction in decoupling was indicated by comparison to the displacement estimated from the elastic theory. It therefore appears that the current heat-sink concept would degrade decoupling, to some degree, at the expense of reducing the cavity size. However, the actual decoupling that could be achieved using the heat sink can be verified only by a nuclear test. Even if the decoupling is reduced below that for a fully decoupled cavity, the quenching technique may be useful for specific requirements for decoupling.

SECTION 4. SPECIFICATIONS FOR A NUCLEAR TEST

4.1 NUCLEAR YIELD

There are two important aspects of the yield to be considered in a nuclear test to determine effectiveness of the heat-sink concept.

4.1.1 Seismic Source

The principal requirement to be met for any seismic decoupling scheme is that the amplitude of teleseismic signals or magnitude be reduced below the threshold of identification as a nuclear explosion. In order to minimize the cost of a proof-test, the scope of the experiment (yield and cavity size) should be as small as possible but sufficient to verify the decoupling technique by means of seismic measurements. Previous cavity decoupling tests have depended upon close-in measurements to determine a displacement potential from which a decoupling factor could be inferred. Near-seismic measurements have also been used. However, it has been recognized that the actual attenuation of teleseismic signals is highly complicated; hence, the most credible decoupling test would employ seismic measurements at large distances.

On the other hand, many seismic recordings of nuclear explosions have been made at the regional stations located only a few hundred kilometers from the Nevada Test Site. Currently, there has been an effort at the Livermore Radiation Laboratory to correlate seismic data recorded at teleseismic stations with those obtained at the regional stations which are about ten times closer in range. Some optimism has been indicated that a correlation of the data can be made. If seismic recordings at the regional stations could be used to predict the amplitudes at teleseismic

distances, then a proof-test of an enhanced cavity-decoupling scheme might be accomplished using a low yield device in a small cavity.

4.1.2 X-Ray Energy

It is anticipated that the application of an enhanced-decoupling scheme might occur where some fraction of the energy release from a nuclear explosion would be in x-ray radiation. Absorption of x-rays by the carbon might affect the flow of the hot gases through the passageways by vaporizing a portion of the carbon near the device. It is not clear whether this might have a beneficial or harmful effect upon the energy quenching process. This effect could not occur in the previous HE experiments.

In a proof-test of the heat-sink principle, it would be recommended that a nuclear device be chosen which emits some fraction of the energy in x-rays.

4.2 CARBON HEAT-SINK CONFIGURATION

4.2.1 Cavity Size

The volume of the cavity required for a proof-test is assumed to be directly proportional to the yield of the test device. HE experiments have shown that quenching has worked over a large range of yield based upon this assumption.

The average bulk density of carbon used in the HE experiments was about 0.5 gm/cm^3. This value, together with the yield, provides a reasonable basis for determining the volume of a cavity which would produce an equilibrium carbon vapor pressure compatible with a practical value of the overburden pressure. As an example, the table in Subsection 2.1 shows the cavity volume and mass of carbon required to reduce the cavity pressure to about 100 bars

for a yield of 1 KT. The cavity volume and carbon weight would be scaled proportional to the yield actually used. These values should be regarded as only approximations due to the uncertainty in the equation-of-state of carbon, volatiles present, and expansion of the cavity due to the impulse delivered to the cavity wall by the carbon impact.

4.2.2 Sources of Carbon

Three forms of carbon with different physical properties have been tested in previous heat-sink experiments. Graphite powder, large chunks of metallurgical coke, and petroleum coke have been used for the heat absorber material. Graphite contained less volatile material; however, it is more costly than the other forms. Metallurgical coke contained the highest percentage of volatile materials, while petroleum coke was somewhat less pure than the graphite. Petroleum coke appears to be readily available in quantity for a proof-test according to a vendor of carbon products.

Chemical analysis of samples for impurities would be recommended prior to a proof-test.

4.2.3 Forming Void Space

During the HE experiments, void spaces throughout the carbon were found necessary for proper mixing of the hot gases with the carbon. Two methods were used, depending upon the form of the carbon. In those experiments using finely divided graphite powder or coke, air cells (balloons, etc.) were dispersed throughout the carbon during loading. The second method was to make use of the natural spacing which occurs when stacking large chunks of coke.

Both methods present new problems to be considered in a proof-test. Since it is necessary to scale up the dimensions of the void spaces in proportion to the cavity size for proper gas flow, special techniques may be required to provide large voids which will support the weight of the surrounding carbon.

4.2.4 Coke Chunks

Results from the HE experiments are used to provide an empirical relation between the cavity size and void dimensions. In the experiments using coke chunks, the minimum recommended ratio of void size-to-cavity diameter was found to be about 1:18. In applying this value to a nuclear test, the coke dimensions can be written

$$\text{Dcoke} = \frac{\text{Dcavity}}{18} W^{1/3} \text{ (KT)}.$$

As an example, the diameter of the cavity for 1 (KT) is about 40 ft. Coke chunks about 2 ft in size would be required according to the relation above. It is not clear that coke can be produced in chunks this size. Further investigation would be required to determine the feasibility of producing large chunks of coke.

4.2.5 Balloons

Plastic balloons used in the HE tests provided a more flexible control of the void size when graphite powder or small petroleum coke was used. One particular problem which arose was that fine particulate carbon produces a buoyant force upon the balloons. During loading of the chamber, the balloons had to be restrained to prevent floating.

This problem was solved by initially filling the chamber from the top with balloons. The natural spacing provided

approximately the correct void size. The coke was small enough to be poured from the port at the top and flow freely through the interstices between the balloons. As the buoyancy increased at the bottom of the chamber, the balloons were held in place by the restraint created by the top half of the chamber. An additional advantage of the technique was that no manned entry was necessary during loading. This would be particularly useful on a proof-test.

Flexibility in the choice of the balloon size might also simplify the construction of the heat-sink. Increasing the size would reduce the number required as long as the diameter is small compared to that of the cavity. It is easily shown that the approximate number $\underline{N}$ required to fill the cavity is given by

$$N = \frac{1}{2}\left(\frac{\text{cavity radius}}{\text{balloon radius}}\right)^3$$

since it has been demonstrated that about one half of the volume of the cavity is occupied by the balloons. In the case of a 1-kT test with a 40-ft cavity filled with 6-ft diameter balloons, 150 would be required. Reducing the size to 3 ft would require 1200.

An additional advantage of larger balloons is that the size of the interstices between adjacent balloons increases with the diameter, affording easier downward flow of the carbon during loading.

Several problems become apparent upon considering the use of balloons in a large-yield test. Reliability of the balloons to remain inflated until test execution is to be considered. Surface loading by the carbon would require preliminary tests to determine the strength of the balloon

material necessary to maintain the load pressures. Pressure monitoring of some balloons would indicate the pressure produced inside the balloons due to the carbon.

An investigation was made on the strength properties of balloon materials commercially available [14]. Materials were found which are used in the manufacture of large balloons, air-supported storage structures, and other applications with high material strength requirements. Tensile strength as high as 450 lb/inch were quoted. Some estimates made on this basis indicate that the strength requirements could be met, at least on a proof-test.

Another question to be raised concerning the use of balloons is the effect of volatile material introduced into the cavity. An estimate was made, based upon data received from Reference 14, of the pressure that would be produced in the cavity due to vaporization of the balloons. Assuming that 150 balloons, 6-ft in diameter are used, the total weight of the balloon material would be 2100 lb compared to the same weight of air in the cavity. The partial pressure of the volatiles are, to a first approximation, the same as air which is only about 17 bars at 4000° K.

Figure 9 illustrates the configuration of a heat sink using balloons for void spaces.

4.2.6 Suspension Support

The problems as indicated in the use of balloons as voids for large cavities arise due to the weight of the carbon which must be supported by the pressure in the balloons. An alternative scheme, which might be considered, would be to support the carbon in some form of container suspended by cables from rock bolts located in the roof of the cavity. Several containers could be spaced along a single cable. By

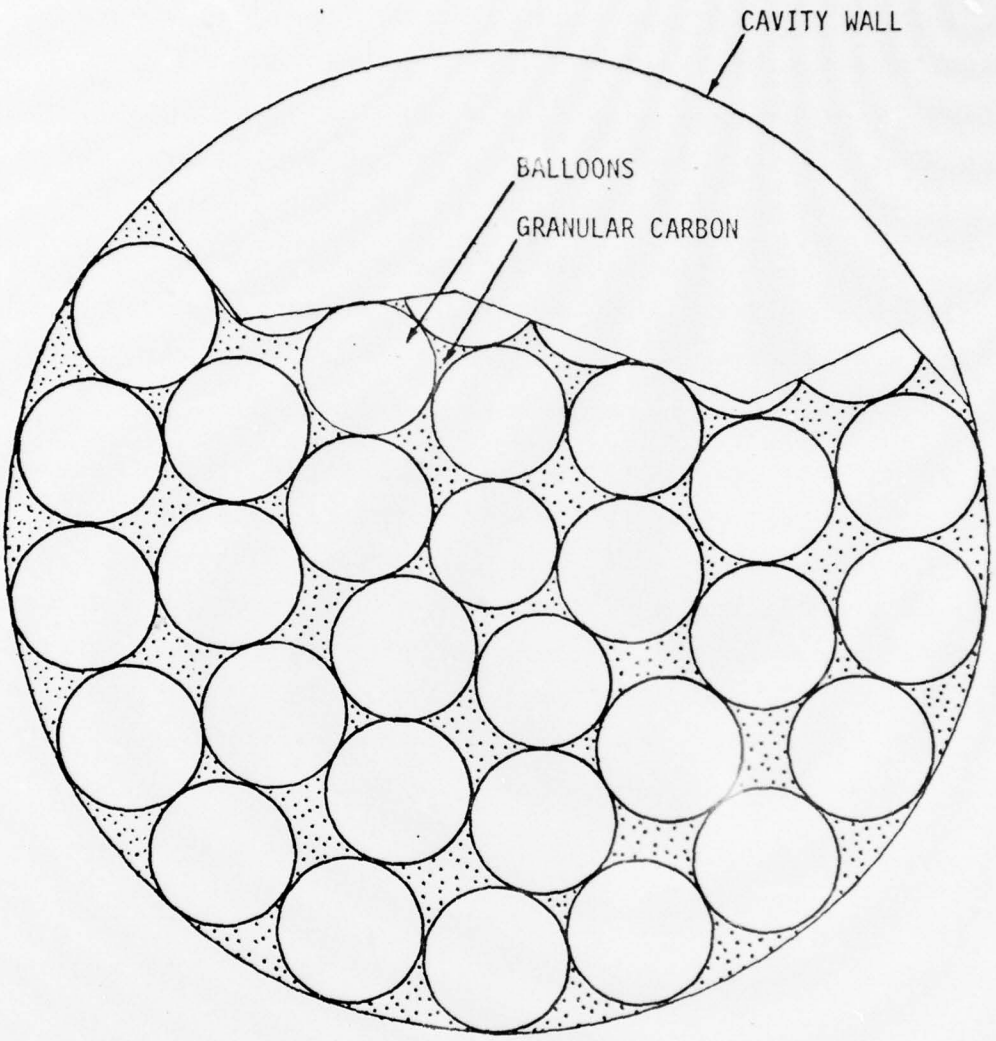

Figure 9. Schematic Illustration of Heat-Sink

staggering the positions of the containers along adjacent cables, the void space between the containers could be made uniform throughout the cavity.

This scheme has not been previously studied and cost effectiveness might rule out its practical use.

Prior to DIAMOND DUST, suspension of large weights from the roof of a cavity were studied in connection with the DIAMOND DUST concept for energy quenching [15].

Another feature which would reduce the number of carbon containers required would be to use a form of carbon of higher density than that used in the current schemes considered.

4.3 SUMMARY OF BASIC DESIGN SPECIFICATIONS

A list of the specifications recommended for planning a nuclear test of the heat-sink concept are listed below. The parameters are chosen to minimize cavity volume based upon the theoretical equation-of-state of carbon and an assumed vapor pressure. The carbon vapor pressure cannot be definitely specified due to the uncertainty in the equation-of-state. Parameter values are based upon a 1-KT yield from which scaling is applied.

Cavity radius	$6.2\ \text{m} \times W^{1/3}\ (\text{KT})$
Cavity volume	$1000\ \text{m}^3 \times W\ (\text{KT})$
Cavity pressure	$\sim$100 bars (complete mixing)
Mass of carbon	0.6 kt/KT yield
Number of balloons (if used)	$\frac{1}{2}\left(\frac{\text{cavity radius}}{\text{balloon radius}}\right)^3$
Size of coke chunks (if used)	$0.6\ \text{m} \times W^{1/3}\ (\text{KT})$

4.4 BASIC MEASUREMENTS

4.4.1 Seismic Measurements

The most important measurements required to determine the effectiveness of the heat sink on seismic decoupling are seismic recordings at stations where previous records from tamped explosions for comparison have been obtained.

4.4.2 Close-In Ground Motion

Measurements of the cavity-wall displacement would be useful for comparison of the cavity volume growth with measured cavity volumes from tamped explosions.

Permanent radial ground displacement in the elastic region might provide data to estimate seismic source strength from the displacement potential.

4.4.3 Cavity Pressure versus Time

Measurement of the pressure in the cavity, together with the cavity-wall displacement, would aid in determining the amount of energy absorbed by the carbon.

4.4.4 Close-In Ground Stress Measurements

Ground stress-time measurements would provide data on the attenuation of the sharp pressure spike produced at the cavity wall by the carbon impact.

4.5 NUMERICAL SUPPORT CALCULATIONS

Numerical calculations of the ground motion produced outside the cavity by a quenched explosion would provide data to be used in guage implacement. Details of the model for quenching to be used in the calculations should be carefully examined and discussed prior to the start of the computations.

Several calculations with variations in shear failure of the ground medium and depth of burial (overburden pressure) would provide guidance in the choice of the rock medium in which the test would be conducted.

4.6 GROUND MEDIUM FOR DECOUPLING

Previous studies on cavity decoupling have shown that maximum decoupling would be achieved in a cavity sufficiently large that only elastic motion of the medium would occur. Also, hard rock such as granite or salt having a large shear modulus would be the best medium for decoupling.

It is not clear, however, that hard rock is the best medium when using the quenching technique discussed in this report. The large impulse on the cavity wall will produce inelastic motion which would be rapidly attenuated. Porous rock generally attenuates strong shocks more rapidly than hard compact media. These questions should be studied prior to choosing the ground medium for testing the decoupling concept.

REFERENCES

1. J. E. Whitener, Technical Directors Final Summary Report, Shot DIAMOND DUST. (Private communication.)

2. J. E. Whitener, Technical Directors Final Summary Report, Shot DIAMOND MINE. (Private communication.)

3. J. E. Whitener, Technical Director's Preliminary Review Report (U), PRR-6821, Defense Nuclear Agency, May 1974.

4. H. R. Kratz and R. E. Rinehart, An Experimental Investigation of Graphite Heat Sinks for Decoupling Underground Nuclear Explosives, Defense Nuclear Agency, 3034, November 1972.

5. R. E. Rinehart, H. R. Kratz et al., Investigation of Heat-Sink Concepts for Containment of Underground Nuclear Explosions, Defense Nuclear Agency, 3154F, November 1973.

6. A. L. Latter et al., "A Method of Concealing Underground Nuclear Explosions," Journal of Geophysical Research, Vol. 66, March 1961.

7. F. R. Gilmore, private communication, R & D Associates.

8. J. F. Krieger, The Thermodynamics of the Graphite-Carbon Vapor System, RM3326, The Rand Corporation, September 1962.

9. J. F. Krieger, The Thermodynamics of the Graphite-Carbon Vapor System, RM3326-1, The Rand Corporation, December 1965.

10. J. F. Krieger, The Thermodynamics of the Graphite-Carbon Vapor System, RM3326-3, The Rand Corporation, October 1969.

11. H. L. Brode, unpublished results using the Harold code, written at The Rand Corporation, January 1969.

12. S. Schuster, R. L. Milton, unpublished results using the AFTON code, R & D Associates, October 1974.

13. G. C. Werth, R. F. Herbst, D. L. Springer, "Amplitudes of Seismic Arrivals from the M Discontinuity," Journal of Geophysical Research, Vol. 67, No. 4, Lawrence Radiation Laboratory, April 1962.

14. Private communication, Muehleisen Manufacturing Co., El Cajon, California, August 1974.

15. Preliminary Feasibility Study, No. 3, DIG HARD, Test Command, Defense Atomic Support Agency, September 1968.

DISTRIBUTION LIST

DEPARTMENT OF DEFENSE

Director
Defense Advanced Research Project Agency
ATTN: Carl Romney
5 cy ATTN: NMRO

Director
Defense Intelligence Agency
ATTN: Weapons & Systems Office

Director
Defense Nuclear Agency
ATTN: TISI
ATTN: DDST
3 cy ATTN: TITL

Under Secretary of Def. for Rsch. & Engineering
ATTN: S&SS (OS)

Defense Documentation Center
Cameron Station
12 cy ATTN: TC

Commander, Field Command
Defense Nuclear Agency
ATTN: FCPR

Chief Livermore Division, Field Command, DNA
Lawrence Livermore Laboratory
ATTN: FCPRL

Assistant to the Secretary of Defense
Atomic Energy
ATTN: Donald R. Cotter

DEPARTMENT OF THE ARMY

Commander
Harry Diamond Laboratories
ATTN: DELHD-OCC
ATTN: DELHD-NP

DEPARTMENT OF THE NAVY

Officer-in-Charge
Naval Surface Weapons Center
ATTN: Code WA501

DEPARTMENT OF THE AIR FORCE

AF Weapons Laboratory, AFSC
ATTN: SUL

AFTAC
3 cy ATTN: B. G. Brooks

DEPARTMENT OF ENERGY

Los Alamos Scientific Laboratory
ATTN: Rpt. Library
ATTN: John McQueen
ATTN: John Hopkins

DEPARTMENT OF ENERGY (Continued)

Sandia Laboratories
ATTN: W. Weart
ATTN: Carter Broyles

Department of Energy
Albuquerque Operations Office
ATTN: Doc. Con. for Library

Department of Energy
Nevada Operations Office
ATTN: Doc. Con. for Library
ATTN: R. Thalgott

University of California
Lawrence Livermore Laboratory
ATTN: Douglas Stephens
ATTN: Richard Wagner
ATTN: Howard Rodean
ATTN: Doc. Con. for Library

Division of Military Applications
ATTN: Robert T. Duff

DEPARTMENT OF DEFENSE CONTRACTORS

Applied Theory, Inc.
ATTN: John Trulio

California Institute of Technology
ATTN: T. J. Ahrens

General Electric Company
TEMPO-Center for Advanced Studies
ATTN: DASIAC, W. Chan

Physics International Company
ATTN: Charles Godfrey

R&D Associates
ATTN: Albert L. Latter
ATTN: Harold L. Brode
ATTN: Ernest A. Martinelli
ATTN: Jack E. Whitener

The Rand Corporation
ATTN: C. C. Mow

SRI International
ATTN: George Abrahamson
ATTN: Douglas Keough

Systems, Science & Software, Inc.
ATTN: Howard Kratz
ATTN: Ted Cherry

Texas A&M University System
c/o Texas A&M Research Foundation
ATTN: John Handin

TRW Defense and Space Systems Group
ATTN: Robert L. Johnson

DEPARTMENT OF DEFENSE CONTRACTORS (Continued)

Weidlinger Associates, Consulting Engineers
ATTN: Melvin Baron

DEPARTMENT OF DEFENSE CONTRACTORS (Continued)

Pacific-Sierra Research Corporation
ATTN: Frank J. Thomas